

## Cell prestress. II. Contribution of microtubules

DIMITRIJE STAMENOVIĆ,<sup>1</sup> SRBOLJUB M. MIJAILOVICH,<sup>2</sup>  
IVA MARIJA TOLIĆ-NØRRELYKKE,<sup>2,3</sup> JIANXIN CHEN,<sup>2</sup> AND NING WANG<sup>2</sup>  
<sup>1</sup>*Department of Biomedical Engineering, Boston University, Boston 02215;* <sup>2</sup>*Physiology Program, Department of Environmental Health, Harvard School of Public Health, Boston, Massachusetts 02115;* and <sup>3</sup>*Rugjer Bošković Institute, 10001 Zagreb, Croatia*

Received 15 June 2001; accepted in final form 24 October 2001

**Stamenović, Dimitrije, Srboljub M. Mijailovich, Iva Marija Tolić-Nørrelykke, Jianxin Chen, and Ning Wang.** Cell prestress. II. Contribution of microtubules. *Am J Physiol Cell Physiol* 282: C617–C624, 2002. First published October 31, 2001; 10.1152/ajpcell.00271.2001.—The tensegrity model hypothesizes that cytoskeleton-based microtubules (MTs) carry compression as they balance a portion of cell contractile stress. To test this hypothesis, we used traction force microscopy to measure traction at the interface of adhering human airway smooth muscle cells and a flexible polyacrylamide gel substrate. The prediction is that if MTs balance a portion of contractile stress, then, upon their disruption, the portion of stress balanced by MTs would shift to the substrate, thereby causing an increase in traction. Measurements were done first in maximally activated cells (10  $\mu$ M histamine) and then again after MTs had been disrupted (1  $\mu$ M colchicine). We found that after disruption of MTs, traction increased on average by  $\sim$ 13%. Because in activated cells colchicine induced neither an increase in intracellular  $Ca^{2+}$  nor an increase in myosin light chain phosphorylation as shown previously, we concluded that the observed increase in traction was a result of load shift from MTs to the substrate. In addition, energy stored in the flexible substrate was calculated as work done by traction on the deformation of the substrate. This result was then utilized in an energetic analysis. We assumed that cytoskeleton-based MTs are slender elastic rods supported laterally by intermediate filaments and that MTs buckle as the cell contracts. Using the post-buckling equilibrium theory of Euler struts, we found that energy stored during buckling of MTs was quantitatively consistent with the measured increase in substrate energy after disruption of MTs. This is further evidence supporting the idea that MTs are intracellular compression-bearing elements.

cytoskeleton; compression; energy; traction; tensegrity

MICROTUBULES (MTs) are structural components of the cytoskeleton that determine cell shape and polarity and that, in cooperation with the actomyosin network, facilitate processes such as cell locomotion and cytokinesis (cf. Refs. 1, 5). Although mechanical measurements in vitro indicate that MTs have high flexural rigidity, which suggests that they may support substantial longitudinal mechanical compression (9, 24, 38), it is not clear whether MTs play a similar role in

living cells. The idea that MTs may support a substantial compression as they balance cytoskeleton contraction has become prominent with the emergence of the cellular tensegrity hypothesis (cf. Refs. 15–17). According to this hypothesis, the synergy of contraction and compression forces is essential for normal cellular function. Thus it is of considerable interest to investigate whether MTs do indeed play the role of compression-supporting elements of the cytoskeleton.

A number of previous observations appear to be consistent with the idea that MTs of living cells carry compression. First, for example, in response to cell contraction and mechanical perturbations, MTs buckle (40, 44). Second, in response to disruption of MTs, cells contract (3, 8, 25, 32, 34). Third, there is evidence of compression-induced MT disassembly in cultured smooth muscle cells (33). On the other hand, data from a recent study on cultured fibroblasts (12) suggests that MT-based cytoskeleton exhibits a fluid-like behavior in response to externally applied mechanical disturbance. Furthermore, it has been shown that nocodazole, a chemical that disrupts MTs, causes an increase in myosin phosphorylation in fibroblasts (22) and an increase in the intracellular  $Ca^{2+}$  in vascular smooth muscle cells (30). Consequently, the observed increase in cell contractility in response to nocodazole could be primarily a result of these responses and not a result of the loss of the load-supporting capacity of MTs. Thus the controversy about the role of MTs as a compression-supporting structure of the cytoskeleton needs to be resolved.

In this study, we attempted to elucidate whether MTs indeed carry a substantial compression as they balance cell contraction. We performed quantitative measurements of indices of MT compression in cultured human airway smooth muscle (HASM) cells by utilizing the traction force microscopy technique (42). We analyzed data from these measurements using a novel energetic approach. We found that in cultured HASM cells, compression of MTs balances a significant but relatively small fraction of cell contractile stress during cell maximal activation by histamine.

Address for reprint requests and other correspondence: D. Stamenović, Dept. of Biomedical Engineering, Boston Univ., 44 Cummington St., Boston, MA 02215 (E-mail: dimitrij@engc.bu.edu).

The costs of publication of this article were defrayed in part by the payment of page charges. The article must therefore be hereby marked "advertisement" in accordance with 18 U.S.C. Section 1734 solely to indicate this fact.

## MATERIALS AND METHODS

Traction force microscopy has been used to measure cell traction at the cell-substrate interface (4, 7, 31). From those measurements, one also can calculate the elastic energy stored in a flexible substrate during cell contraction (4). In our companion study (42), we used this technique to measure traction of cultured HASM cells in response to agonist-induced cell contraction. In the present study, we utilized this technique to assess compression in MTs in these cells.

Our working hypothesis is that cell contraction is balanced partly by traction at the cell-substrate interface and partly by compression of MTs (Fig. 1). To test this hypothesis, we used traction force microscopy to measure cell traction in stimulated cultured HASM cells before and after cell MTs were treated by colchicine, a drug that disrupts MTs. If this hypothesis holds, then for a given state of contraction, we predicted that after disruption of MTs 1) traction would increase due to a transfer of the part of the contractile stress balanced by MTs to the substrate and 2) energy stored in the substrate would increase due to transfer of the compression energy of MTs to the substrate. Formal definitions of the contractile stress, traction, and stored energy are given later in the text.

**Cell culture.** HASM cells were cultured ( $10^5$  cells/cm<sup>2</sup>) with Ham's F-12 medium supplemented with 10% fetal bovine serum, 50 mg/ml gentamicin, and 2.5  $\mu$ M/ml amphotericin B. Cells at passages 3–6 were used for all experiments. After they reached confluence, cells were serum deprived for 48 h and then plated in serum-free defined medium. Cells were plated sparsely on a 70- $\mu$ m-thick polyacrylamide elastic gel block coated with collagen type I (0.2 mg/ml). More details about cell culture can be found in our companion paper (42). We chose HASM cells because we showed previously that in this cell type, we can pharmacologically modulate cell contraction in a dose-dependent manner (13).

**Traction force microscopy.** A detailed description of this technique is given in our companion paper (42). Briefly, the polyacrylamide gel substrate was used as a strain gauge to measure the interfacial cell-substrate traction. Many fluorescent microbeads (0.2- $\mu$ m diameter) embedded near the gel apical surface served as markers whose displacements were recorded as the adhering cell contracted. The bottom surface of the gel was covalently bonded to a flat, rigid plate, and the lateral surfaces were free. From bead displacements and known elastic properties of the gel (Young's modulus values of 870 and 1,300 Pa and a Poisson's ratio of 0.48), the traction was calculated as described in Refs. 4 and 42.

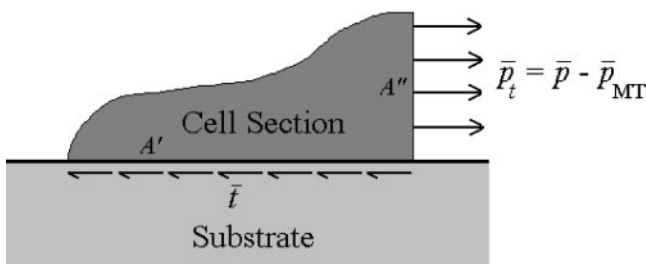


Fig. 1. A free-body diagram of a section of the cell adhering to the substrate. The traction force is balanced by the net prestress force:  $\bar{p}_t = \bar{t} A'/A''$ , where  $\bar{t} = (1/A'') \int_{A'} \mathbf{t} \cdot \mathbf{n} dA$  is the mean traction,  $\bar{p}_t$  is the corresponding mean prestress,  $A'$  and  $A''$  are the projected and the cross-sectional areas of the cell section, respectively,  $\mathbf{t}$  is the traction vector field, and  $\mathbf{n}$  is the unit outer normal vector to  $A''$ . Note that  $\bar{p}_t$  equals the net contractile prestress  $\bar{p}$  reduced by the part of the prestress ( $\bar{p}_{MT}$ ) balanced by microtubules (MTs),  $\bar{p}_t = \bar{p} - \bar{p}_{MT}$ .

**Protocol.** HASM cells plated on a polyacrylamide gel block were first treated with 10  $\mu$ M histamine, then with 1  $\mu$ M colchicine plus 10  $\mu$ M histamine, and, finally, with trypsin. This dose of histamine was shown to produce maximum increases in cell stiffness and myosin light chain phosphorylation. Histamine was added with colchicine to maintain the saturated bath concentration. Trypsin was added until a cell was completely detached from the substrate. Note that before the saturated dose of histamine was added, cells were treated with lower dosages (over 4 min) for the purpose of studies described in our companion paper (42).

Images of fluorescent microbeads were taken at baseline, at 40-s intervals after histamine addition, after colchicine addition, and, finally, after trypsin addition. The image after trypsin was used as the reference (traction-free) image. The displacement field ( $\mathbf{u}$ ) was calculated as follows:  $\mathbf{u}$  at baseline, after histamine addition, and after colchicine addition was obtained by cross-correlating the corresponding image with the reference image. A detailed description of how  $\mathbf{u}$  was calculated is given in Ref. 4. The displacement field  $\mathbf{u}$  was then used to calculate the corresponding traction vector field ( $\mathbf{t}$ ) as described in Refs. 4 and 42; local traction was defined as a local contact force between the cell and the substrate per unit local contact surface area.

**Calculation of traction, strain energy stored in the substrate, and the prestress.** The mean traction ( $\bar{t}$ ) was obtained as the root mean square of  $\mathbf{t}$  over the cell projected area ( $A'$ ) (4). The strain energy ( $W_t$ ) stored in the substrate was calculated as the work of  $\mathbf{t}$  on  $\mathbf{u}$  (4)

$$W_t = \frac{1}{2} \int_{A'} \mathbf{t} \cdot \mathbf{u} dA \quad (1)$$

The contractile stress ("prestress") was defined as the net force transmitted across a cross-sectional area of the cell by the cytoskeleton contractile network per unit area. According to our hypothesis, the mean prestress ( $\bar{p}$ ) is the sum of two parts: one balanced by traction ( $\bar{p}_t$ ) and the other by compression of MTs ( $\bar{p}_{MT}$ )

$$\bar{p} = \bar{p}_t + \bar{p}_{MT} \quad (2)$$

We calculated  $\bar{p}_t$  from measurements of  $\mathbf{t}$ , using a free-body diagram of a cell section (Fig. 1), as  $\bar{p}_t = (1/A'') \int_{A'} \mathbf{t} \cdot \mathbf{n} dA$ , where  $A'$  and  $A''$  are the projected and cross-sectional areas of the cell section, respectively, and  $\mathbf{n}$  is the unit outer normal vector to  $A''$ . This means that only the component of the net traction force normal to the cross-sectional area is balanced by the prestress. For a single cell,  $\bar{p}_t$  was calculated for many cell cross sections (at  $\sim 2.7$ - $\mu$ m intervals), and the average value was obtained. More details about these computations can be found in our companion paper (42). According to Eq. 2, for a given  $\bar{p}$ , disruption of MTs (i.e.,  $\bar{p}_{MT} \rightarrow 0$ ) would cause an increase in  $\bar{p}_t$  by the amount equal to  $\bar{p}_{MT}$ . Thus  $\bar{p}_{MT}$  was obtained as a change in  $\bar{p}_t$  after colchicine addition relative to histamine, i.e.,  $\bar{p}_{MT} = \Delta \bar{p}_t$ , where  $\Delta$  symbolizes change.

**Immunofluorescence staining of MTs.** To find out how depolymerization of MTs in response to colchicine progressed with time, we serum deprived HASM cells for 24 h before they were plated overnight in a defined medium on type I collagen-coated (5  $\mu$ g/ml) Lab-Tek chamber slides. The cells were treated with colchicine (1  $\mu$ M) for 1, 3, 5, 10, and 15 min and then fixed, permeabilized, and stained using indirect immunofluorescence methods as described in Ref. 29.

**Data analysis.** Statistical differences were assessed by the paired *t*-test. Differences with  $P < 0.05$  were considered significant.

Table 1. Changes in traction, energy, and prestress after colchicine

Cell No.	Traction Change, Pa	Energy Change, pJ	Prestress Change, Pa
1h	13.29	0.016	184
2h	5.70	0.058	294
3h	43.18	0.281	815
4h	24.08	0.201	150
5s	38.92	0.183	283
6s	-3.07	-0.021	158
7s	48.33	0.324	297
8s	13.16	0.073	194
9s	13.00	0.049	78
10s	5.13	0.061	48
11h	9.34	0.020	98
12h	38.84	0.209	436
13h	50.14	0.189	712
Mean	23.08	0.126	288
SE	5.11	0.030	66

Results are changes in the root mean square traction ( $\Delta\bar{t}$ ), in the energy stored in the substrate ( $\Delta W_t$ ), and in the mean prestress ( $\Delta\bar{p}_t$ ) obtained from traction force microscopy measurements on cultured human airway smooth muscle cells in controls, after addition of 10  $\mu$ M histamine and 1  $\mu$ M colchicine ( $n = 13$  cells). Letters next to the cell number indicate the measurements done on hard (h) polyacrylamide gels with a Young's modulus of 1,300 Pa and on soft (s) gels with a Young's modulus of 870 Pa.

## RESULTS

Measurements were done on  $n = 13$  cells. Six of those cells were plated on a soft gel (Young's modulus of 870 Pa) and seven on a stiff gel (Young's modulus of 1,300 Pa). No significant difference between data obtained from these two gels was observed, and therefore all data have been combined. Here we have presented the data from the point when the traction reached its peak ( $\sim 3$  min after histamine addition and 3–5 min after colchicine addition). In most cells,  $\bar{t}$  and  $W_t$  increased after histamine addition and increased further after colchicine addition (Table 1); the average increases in  $\bar{t}$  and  $W_t$  after colchicine addition relative to histamine was  $\sim 13\%$  ( $\Delta\bar{t} \approx 23$  Pa) and  $\sim 30\%$  ( $\Delta W_t \approx 0.13$  pJ), respectively. All of these increases were significant ( $P < 0.05$ ). The increases in  $\bar{t}$  and  $W_t$  after

histamine were expected as a result of increased contractility due to the stimulation of the cell actomyosin apparatus (42). The increases in  $\bar{t}$  and  $W_t$  in response to colchicine were not a result of increased myosin light chain phosphorylation due to MT depolymerization (40). They also were not a result of increased intracellular  $\text{Ca}^{2+}$  in response to colchicine treatment; measurements showed that there was no increase in the intracellular  $\text{Ca}^{2+}$  in histamine maximally activated HASM cells after colchicine addition (40). Thus we concluded that the observed increase in  $\bar{t}$  and  $W_t$  after colchicine addition resulted from the loss of the compression-supporting capacity MTs, which balanced a part of cell contractile stress before their disruption. This, in turn, produced a shift of load and energy from MTs to the substrate. It is noteworthy that these data were not consistent with MTs bearing tension; in such a case the disruption of MTs would lead to a decrease in  $\bar{t}$  and  $W_t$  as previously observed when tension-bearing actin filaments were disrupted by cytochalasin D (23).

Results from immunofluorescence staining measurements show that disruption of MTs was evident 3 min after colchicine addition (Fig. 2). The filamentous patterns of MTs gradually started to disappear and MTs became disorganized as treatment duration increased from 3 to 15 min (Fig. 2). Because most of our traction measurements were done 3–5 min after colchicine addition, it is apparent that structural integrity of a substantial fraction of MTs was disrupted by this time. However, a fraction of MTs remained intact even 15 min after colchicine addition (Fig. 2). Note that the images in Fig. 2 serve only as a qualitative indicator that MTs started to disassemble within the duration of traction measurements.

We also calculated  $\bar{p}_t$ , i.e., the component of the prestress balanced by the traction, using the algorithm described in our companion paper (42). We found that  $\bar{p}_t$  increased after MT disruption by colchicine (Table 1). We interpreted this increase in  $\bar{p}_t$  as a part of the prestress balanced by MTs (i.e.,  $\Delta\bar{p}_t = \bar{p}_{\text{MT}}$ ). On average,  $\bar{p}_t$  changed by  $\Delta\bar{p}_t \approx 288$  Pa, which is  $\sim 14\%$  of  $\bar{p}_t$

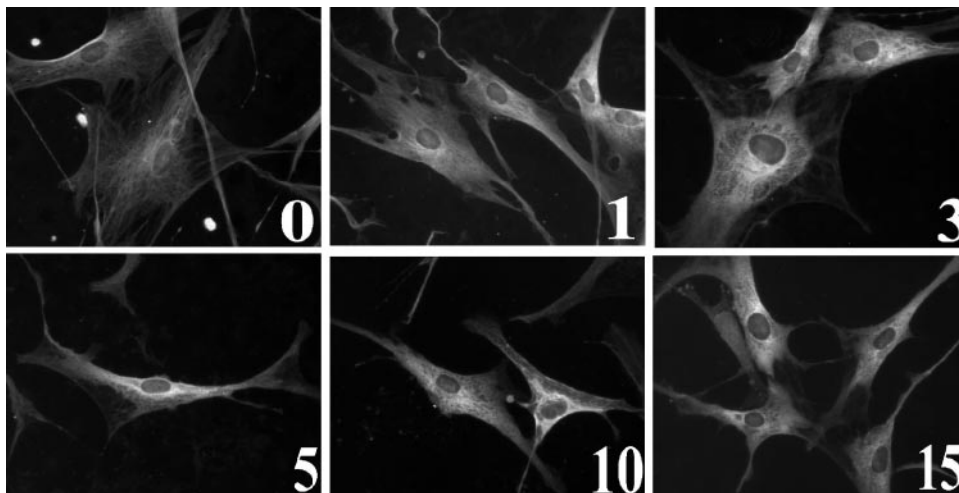


Fig. 2. Immunofluorescence staining of MTs of human airway smooth muscle (HASM) cells for 1, 3, 5, 10, and 15 min after addition of colchicine (1  $\mu$ M). Disruption of the MT network was visible 3 min after colchicine was added. The filamentous patterns of MTs gradually started to disappear, and MTs became disorganized as treatment duration increased from 3 to 15 min. Because most of our traction measurements were done 3–5 min after colchicine addition, it is apparent that structural integrity of a substantial fraction of MTs was disrupted by this time.

(Table 1); i.e., MTs balanced  $\sim 14\%$  of the prestress. Data from individual cells showed that this contribution of MTs ranged from  $\sim 3$  to  $30\%$ .

Together, the above results show that disruption of MTs by colchicine caused significant increases in  $\bar{t}$  and  $W_t$ . These findings were consistent with our hypothesis that cytoskeleton-based MTs support compression.

We next investigated whether the observed increase in the energy stored in the gel substrate after the colchicine treatment,  $\Delta W_t \approx 0.13$  pJ (Table 1), could be accounted for by the compression energy ( $W_{MT}$ ) stored in MTs before their disruption. To obtain  $W_{MT}$ , we used a theoretical approach based on an energetic analysis.

**Energetic considerations.** Our working hypothesis predicts that if MTs indeed carry compression and if there is no energy loss during MT disruption, then  $W_{MT} = \Delta W_t$ .

We first used the data for  $\Delta \bar{p}_t \approx 288$  Pa to calculate the corresponding compression stress ( $S_{MT}$ ) carried by individual MTs before disruption (recall that  $\Delta \bar{p}_t = \bar{p}_{MT}$ ). From the mechanical balance between  $S_{MT}$  and  $\bar{p}_{MT}$  (i.e., between compression and contraction), one can show that  $\bar{p}_{MT} \propto \phi_{MT} S_{MT}$ , where  $\phi_{MT} \approx 0.19\%$  is the volumetric fraction of MTs in the cell (35). We assumed that  $\bar{p}_{MT} = \phi_{MT} S_{MT}$ , which corresponds to the case where MTs are perpendicular to the cell cross-sectional area  $A''$ , and obtained  $S_{MT} \approx 152$  kPa.

To calculate  $W_{MT}$ , we depicted MTs of the cytoskeleton as slender, cylindrical elastic rods supported laterally by intermediate filaments (IFs), as proposed by Brodland and Gordon (2). This support is needed because long, slender MTs would easily buckle and collapse under compression stress  $S_{MT}$ . If, however, MTs were supported by IFs, they would not collapse even if  $S_{MT}$  exceeded a critical buckling value. Instead, MTs would attain a postbuckling equilibrium configuration characterized by a wavy, sinusoidal shape (2, 37). We used this model to calculate  $W_{MT}$  as follows.

We assumed that, within the cell, MTs span the distance  $l$  of  $20 \mu\text{m}$  and that they are stabilized by a continuous elastic lateral support of IFs of stiffness  $q \approx 8$  Pa. These values were chosen on the basis of cell size and based on measurements in vitro on IF gels (18, 27) (see DISCUSSION). Other parameters required for calculation of  $W_{MT}$  were taken from the literature: the bending (flexural) rigidity  $B = 21.5$  pN $\cdot\mu\text{m}^2$ , the cross-sectional area of an MT  $A_{MT} = 190$  nm $^2$  (9), and  $\phi_{MT} \approx 0.19\%$  (35). The average cell volume was estimated to be  $\sim 5,000 \mu\text{m}^3$ . From the above values, we obtained  $W_{MT} \approx 0.18$  pJ using the postbuckling equilibrium theory of Euler elastica (see APPENDIX). This value was close to the measured value of  $\Delta W_t \approx 0.13$  pJ.

## DISCUSSION

Elucidation of biophysical mechanisms by which mechanical stresses are transmitted and balanced within the cell-substrate system is critical for understanding how mechanical signals affect cellular function. Previous studies have shown the role of the substrate in balancing cell contractile stress and how it may affect

cell locomotion, spreading, or apoptosis (6, 11, 31). In this study we obtained for the first time prime quantitative data suggesting that MTs also contribute to the balance of the cell contractile stress. According to our measurements, it appears that in maximally activated HASM cells, MTs contribute  $\sim 3$ – $30\%$  ( $\sim 14\%$  on average) to the balance of the contractile prestress. The rest is balanced by the substrate.

In this study we used a novel energetic approach that had several advantages. First, energy is a scalar quantity, independent of the choice of coordinate system, with the property that the total energy is the sum of energies of various components. This simplified mathematical handling of the data. Second, energy analysis requires minimal specifications about cytoskeleton architecture. Results of the energetic analysis showed that 1) MTs buckle as they carry compression, and 2) IFs may play a stabilizing role in this process. These findings appear to be consistent with previous observations. First, it was observed that MTs of living cells buckle during cell contraction (40, 44). Second, the similarity between the observed wavy shape of buckled MTs of living cells and the shape predicted from the theory (2, 37) suggests that in living cells, MTs are indeed stabilized by the surrounding cytoskeleton structures. Finally, experimental data show that there exists mechanical interlinking between MTs and IFs in fibroblasts (36).

Paul et al. (30) found that the increase in contractility in unstimulated arteries is paralleled by a small increase in intracellular  $\text{Ca}^{2+}$  after colchicine treatment. They concluded that MTs do not significantly contribute to vascular smooth muscle mechanics but play a role in modulating  $\text{Ca}^{2+}$  signal transduction. On the other hand, recent measurements showed that there was no increase in intracellular  $\text{Ca}^{2+}$  in response to colchicine treatment of histamine-activated HASM cells, although colchicine alone induced a small increase in intracellular  $\text{Ca}^{2+}$  in unstimulated HASM cells (40). Consequently, the observed increase in traction, energy, and prestress after colchicine treatment in HASM cells (Table 1) could not be attributed to an increase in intracellular  $\text{Ca}^{2+}$ . These results are consistent with published results in isolated arterioles (32).

A key assumption of this study was that the mechanical equilibrium and the energy budget of the cell-substrate system were maintained by means of a three-way force balance between the contractile elements, cytoskeleton-based MTs, and the substrate. However, it is very likely that other cellular structures also may contribute to the balance of forces and energy budget. First, it was observed recently that stress fibers of endothelial cells exhibit buckling in response to large shortening of the substrate (14), suggesting that they may carry compression. However, stress fibers isolated from fibroblasts and endothelial cells on average shorten to about 23% of their initial lengths, suggesting that under normal physiological conditions stress fibers are indeed in tension (20). Second, we also do not know the contribution of swelling pressure of the cyto-

plasm to the force balance within the cell. However, the contribution of the cytoplasm to the energy budget at steady state is zero because the cytoplasm is virtually incompressible. Third, the contributions of the actin cytoskeleton and myosin cross bridges to the energy budget did not exceed the order of  $10^{-2}$  pJ each (see APPENDIX). These values are at least an order of magnitude smaller than the measured energy  $W_i$  stored in the substrate and the estimated compression energy  $W_{MT}$  stored in MTs. Fourth, on the basis of data from *in vitro* measurements, IF gels have much lower stiffness than actin gels, except at high strains (18), suggesting that the energy stored in IFs is substantially smaller than the energy stored in the actin network, which itself has little contribution to energy storing. Thus we concluded that in the cell-gel substrate system, the MTs and the gel substrate had the most prominent contribution to the energy budget. The other contributions appear to be less important. Nevertheless, their inclusion would somewhat reduce our estimate of the contribution of MTs to the cell energy budget.

It was assumed that there was no energy dissipation in the gel substrate-cell system, i.e., that the system is elastic. Although the gel behavior has been shown to be almost elastic (31), it is not true for HASM cells, which are known to exhibit a dissipative, viscoelastic behavior (13). Nevertheless, all of our measurements were done at the steady state when all viscoelastic stresses are dissipated, and therefore, cellular viscoelasticity should have little effect on data for the traction, energy, and prestress. On the other hand, it is likely that during disruption of MTs by colchicine, a portion of the energy stored in MTs was irreversibly lost. Hence, only a fraction of the energy associated with MTs might be transferred to the substrate, and thus the observed energy increase  $\Delta W_i$  could be an underestimate. This, in turn, may compensate the overestimates caused by our exclusion of the contributions of actin, myosin, and IFs to the energy storage of the cell.

The fact that the traction measured on soft gels (Young's modulus of 870 Pa) did not differ significantly from the values obtained on hard gels (Young's modulus of 1,300 Pa) can be explained as follows. First, gel stiffness varied from experiment to experiment: the soft gel range of stiffness was 860–1,000 Pa, whereas the hard gel range of stiffness was 920–1,600 Pa. Thus in some measurements the gel stiffness was not different at all. Second, Yu-Li Wang's group (39) have shown that an increase in gel stiffness by a factor of  $\sim 2.4$  causes a modest increase in traction of  $\sim 50\%$ . Thus it appears that traction measurements are not very sensitive to changes in the substrate stiffness.

We do not know whether colchicine affects actin polymerization and thus the state of stress within the actin network of HASM cells. Earlier studies showed that colchicine does not cause disruption of actin filaments but does cause a small increase in cytoskeleton-associated actin in leukocytes (21) and a significant increase in filamentous actin in fibroblasts (19). The latter finding corresponds to a 1-h period, whereas the colchicine treatment in our measurements did not ex-

ceed 10 min. This, in turn, suggests that if there were changes in the amount of actin in our measurements, they might not be large.

A critical review of the assumptions of our theoretical analysis is given below. The crudest assumptions of the analysis were the length of MTs of 20  $\mu\text{m}$  and the stiffness of the lateral support of IFs of 8 Pa. With the assumption that the MTs spread outwardly from the cell perinuclear region, and taking into account that the length and width of spread airway smooth muscle cells are roughly 100 and 30  $\mu\text{m}$ , respectively, our assumption that MTs span an average distance of  $\sim 20$   $\mu\text{m}$  was not unreasonable. Furthermore, Brodland and Gordon (2) used the same value in their analysis of MT buckling. The assumed stiffness of IFs of 8 Pa is consistent with *in vitro* measurements on vimentin (18) and keratin (27) gels. In general, vimentin IF contributes about 20% of cytoskeleton stiffness in endothelial cells and fibroblasts (41). However, desmin is the most abundant IF in HASM cells (10), and few data on mechanical properties of desmin in these cells are available. Furthermore, the interlinking between IFs and MTs within the cytoskeleton is facilitated by plectin (36), whose mechanical properties are not known. It is likely that other cytoskeleton structures and the viscoelastic cytoplasm also play a role in stabilizing MTs. Thus the assumed value of 8 Pa of the stiffness of the lateral support is questionable but seems to be a good guess for the following reasons. First, a 25% increase in this value would overly stabilize MTs (i.e., no buckling would occur), which is contrary to previously observed buckled shapes of MTs (40, 44), albeit in cells other than smooth muscle cells. If MTs did not buckle, then the energy associated with their compression would be much smaller (order of  $10^{-4}$  pJ, see APPENDIX) than the measured value of the energy. Second, a 25% decrease in the assumed value of stiffness of the lateral support would result in an  $\sim 2.5$ -fold greater value of  $W_{MT}$  than the measured increase in energy,  $\Delta W_i$ . We also performed an order-of-magnitude analysis of  $W_{MT}$  by using the method described in the APPENDIX and assuming that  $l = O(10^1)$   $\mu\text{m}$ ,  $q = O(10^1)$  Pa,  $B = O(10^1)$  pN $\cdot\mu\text{m}^2$ , and  $A_{MT} = O(10^2)$  nm $^2$ , where  $O(10^x)$  denotes the order of magnitude. We estimated that  $W_{MT} = O(10^{-1}-10^0)$  pJ. The measured value of  $\Delta W_i$  falls within this range.

In conclusion, our study showed that a greater part of contractile stress of cultured HASM cells was balanced by the substrate, but a significant portion of this stress was balanced by the compression-supporting network of MTs. To our knowledge, these are the first prime quantitative experimental data showing that MTs behave as compression-bearing elements as they balance the contractile stress. On the basis of our energetic analysis, we have concluded that MTs buckle as they carry compression and that, in this process, IFs (and possibly other intracellular structures) stabilize MTs.

Our findings and the findings from our companion study (42) have an important implication on the tensegrity idea. Key features of the cellular tensegrity

hypothesis are that the cell stiffness increases in proportion with the cytoskeleton prestress and that the prestress is balanced by intracellular compression-supporting elements (e.g., MTs). Although results from our two studies are consistent with these features, the fact that the MTs balance only a relatively small fraction of the prestress in this spread HASM cell suggests that one may not need to invoke tensegrity to explain the prime feature of contractile cell deformability, i.e., the association of cell stiffness with the cytoskeleton prestress. Consequently, the choice of a model of cell deformability among various prestressed structures (e.g., tensegrity, cable nets, cortical membrane) is likely to depend on the cell type, the extent of cell spreading, or some other factors.

APPENDIX

The energy of buckling of MTs,  $W_{MT}$ , is calculated as follows. MTs were depicted as slender elastic cylindrical rods of length  $l$ , cross-sectional area  $A_{MT}$ , and bending (flexural) rigidity  $B$ , supported by a lateral continuous support of IFs of stiffness  $q$ . This lateral support effectively reduces the critical buckling length ( $L_{cr}$ ) of MTs;  $L_{cr} < l$ . Thus the problem of buckling of a laterally supported strut of length  $l$  reduces to the problem of buckling of a simple Euler pin-ended strut of length  $L_{cr}$  with no lateral support, known as elastica (37). This makes the calculation of buckling energy much simpler.

$L_{cr}$  was obtained from a theoretical relationship (37) shown in Fig. 3 in a graphical form. The graph in Fig. 3 was calculated for  $q = 8$  Pa and  $B = 21.5$  pN· $\mu\text{m}^2$  (9). For  $l = 20$   $\mu\text{m}$ , it was found that  $L_{cr}/l = 0.14$ , and hence  $L_{cr} = 2.8$   $\mu\text{m}$ . This value was then used to calculate the critical buckling stress ( $S_{cr}$ ) for the Euler elastica as  $S_{cr} = (\pi^2 B)/[(L_{cr})^2 A_{MT}]$ , where  $A_{MT} = 190$   $\text{nm}^2$  (9). It was found that  $S_{cr} \approx 142$  kPa.

We next used the theory of postbuckling equilibrium of Euler elastica (37) to calculate  $W_{MT}$ . According to this theory, the buckling is not a catastrophic event, and compressed elastica maintains equilibrium after the compression stress exceeds the critical buckling stress, i.e.,  $S_{MT} > S_{cr}$  (see Fig. 4,

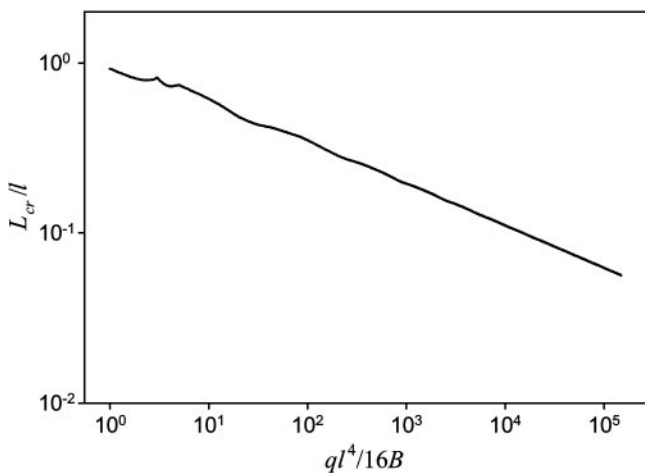


Fig. 3. Relationship between  $L_{cr}/l$  and  $ql^4/16B$ , obtained numerically from the theoretical equation from Ref. 35, where  $L_{cr}$  is the critical buckling length of Euler elastica,  $l = 20$   $\mu\text{m}$  is the assumed length of MTs,  $q = 8$  Pa is the stiffness of the lateral support of intermediate filaments (IFs), and  $B = 21.5$  pN· $\mu\text{m}^2$  is the flexural (bending) rigidity of MTs. This relationship is used to obtain  $L_{cr}$ .

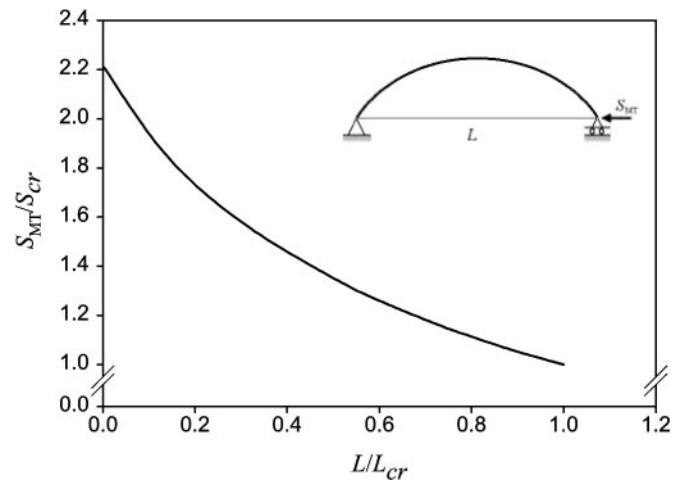


Fig. 4. Universal postbuckling compression vs. chord-length relationship (37) of pin-ended Euler elastica (shown in inset), where  $S_{MT}$  is compression stress,  $S_{cr}$  is critical buckling stress,  $L$  is chord-length (see inset), and  $L_{cr}$  is the critical buckling length of elastica. This relationship is used to obtain the energy per unit volume stored in an MT (Eq. A1).

inset). The universal relationship between the compression stress and the chord length  $L$  of the elastica is given in Fig. 4. The area under the curve corresponds to the energy associated with buckling.

Using the value of  $S_{MT} \approx 152$  kPa determined from the experimental data for prestress (see *Energetic consideration*) and  $S_{cr} \approx 142$  kPa, we obtained  $L/L_{cr} = 0.87$  from Fig. 4. The energy per unit volume ( $w_{MT}$ ) of the elastica was obtained as

$$w_{MT} = S_{cr} \int_1^{L/L_{cr}} (S_{MT}/S_{cr}) d(L/L_{cr}) \tag{A1}$$

By substituting the values of  $S_{cr} \approx 142$  kPa and  $L/L_{cr} = 0.87$  into Eq. A1, we determined from the relation in Fig. 4 that  $w_{MT} \approx 0.018$  pJ/ $\mu\text{m}^3$ . The energy stored in the cytoskeleton-based MTs was then calculated as  $W_{MT} = \phi_{MT} V w_{MT}$ , where  $\phi_{MT} \approx 0.19\%$  is the volumetric fraction of MTs in the cell (35) and  $V = 5,000$   $\mu\text{m}^3$  is the cell volume. It was determined that  $W_{MT} = 0.176$  pJ.

If MTs do not buckle but only shorten under compressive stress  $S_{MT} \approx 152$  kPa, the energy stored per unit volume of a single MT is  $(S_{MT})^2/2E_{MT}$ , assuming that MTs are linearly elastic. Here  $E_{MT} \approx 1.2$  GPa is the Young's modulus of a single MT (9). The corresponding energy stored in MTs of the cytoskeleton is  $W_{MT} = \phi_{MT} V (S_{MT})^2/2E_{MT}$ . It was determined that  $W_{MT} \approx 0.9 \times 10^{-4}$  pJ.

The energy stored in the actin network ( $W_{MF}$ ) was calculated as follows. It was assumed that the actin filaments were linearly elastic. In that case, the energy per unit volume of a single actin microfilament is  $(S_{MF})^2/2E_{MF}$ , where  $S_{MF}$  is stress and  $E_{MF} \approx 2.6$  GPa (9) is the Young modulus of the filament. The total energy stored in the actin cytoskeleton is therefore equal to  $W_{MF} = \phi_{MF} V (S_{MF})^2/2E_{MF}$ , where  $\phi_{MF} \approx 0.21\%$  is the volume fraction of actin microfilaments in the cell (cf. Ref. 35) and  $V = 5,000$   $\mu\text{m}^3$  is the cell volume. Stress  $S_{MF}$  was obtained from the data for the net mean prestress = 2,211 Pa (42), assuming that the microfilaments form a three-dimensional randomly oriented network where  $S_{MF} = 3p/\phi_{MF}$  (35). It was found that  $W_{MF} \approx 0.02$  pJ.

The energy stored in the myosin cross bridges ( $W_{CB}$ ) was obtained as follows. The maximum energy per cross bridge is  $e_{CB} = 2.7 \times 10^{-8}$  pJ (26). Thus the total energy stored in

myosin cross bridges of the cell is  $W_{CB} = \phi_{CB} V_{eCB} / v_{CB}$ , where  $\phi_{CB}$  is the volumetric fraction of the cross bridges in the cell,  $v_{CB}$  is the volume of a cross bridge, and  $V = 5,000 \mu\text{m}^3$  is the cell volume. The quantities  $\phi_{CB}$  and  $v_{CB}$  were obtained as follows. The myosin content in the smooth muscle is approximately one-fifth the myosin content in the skeletal muscle cells, which is  $20 \mu\text{M}$  (28), and the myosin mass density was assumed to be that of water. From these data it was obtained that  $\phi_{CB} \approx 0.18\%$ . The crude estimate of  $v_{CB} \approx 10^{-5} \mu\text{m}^3$  was obtained from the data for the cross-bridge geometry (43). Thus it was found that  $W_{CB} \approx 0.024 \text{ pJ}$ .

We thank Dr. Don Ingber for making his laboratory available for performance of some of the experiments.

This work was supported by National Heart, Lung, and Blood Institute Grants HL-65371 and HL-33009 and by National Aeronautics and Space Administration Grant NAG5-4839.

## REFERENCES

- Amos LA and Amos WB. *Molecules of the Cytoskeleton*. New York: Guilford, 1991.
- Brodland GW and Gordon R. Intermediate filaments may prevent buckling of compressively loaded microtubules. *ASME J Biomech Eng* 112: 319–321, 1990.
- Brown RA, Talas G, Porter RA, McGrouther DA, and Estwood M. Balanced mechanical forces and microtubule contribution to fibroblast contraction. *J Cell Physiol* 169: 439–447, 1996.
- Butler JP, Tolić-Nørrelykke IM and Fredberg JJ. Estimating traction fields, moments, and strain energy that cells exert on their surroundings. *Am J Physiol Cell Physiol* 282: C595–C605, 2002.
- Canman JC and Bement WM. Microtubules suppress actomyosin-based cortical flow in *Xenopus* oocytes. *J Cell Sci* 110: 1907–1917, 1997.
- Chen CS, Mrksich M, Huang S, Whitesides GM, and Ingber DE. Geometric control of cell life and death. *Science* 276: 1425–1428, 1997.
- Dembo M and Wang YL. Stress at the cell-to-substrate interface during locomotion of fibroblasts. *Biophys J* 76: 2307–2316, 1999.
- Gills JP, Roberts BC, and Epstein DL. Microtubule disruption leads to cellular contraction in human trabecular meshwork cells. *Invest Ophthalmol Vis Sci* 39: 653–658, 1998.
- Gittes F, Mickey B, Nettleton J, and Howard J. Flexural rigidity of microtubules and actin filaments measured from thermal fluctuations in shape. *J Cell Biol* 120: 923–934, 1993.
- Halayko AJ, Salari H, Ma X, and Stephens NL. Markers of airway smooth muscle cell phenotype. *Am J Physiol Lung Cell Mol Physiol* 270: L1040–L1051, 1996.
- Harris AK, Wild P, and Stopak D. Silicon rubber substrata: a new wrinkle in the study of cell locomotion. *Science* 208: 177–179, 1980.
- Heidemann SR, Kaeche S, Buxbaum RE, and Matus A. Direct observations of the mechanical behaviors of the cytoskeleton in living fibroblasts. *J Cell Biol* 145: 109–122, 1999.
- Hubmayr RD, Shore SA, Fredberg JJ, Planus E, Panettieri RA Jr, Moller W, Heyder J, and Wang N. Pharmacological activation changes stiffness of cultured airway smooth muscle cells. *Am J Physiol Cell Physiol* 271: C1660–C1668, 1996.
- Hucker W, Yin FCP, and Costa KD. The role of cytoskeletal tension in maintaining actin stress fiber integrity (Abstract). *Ann Biomed Eng* 28: S-65, 1999.
- Ingber DE. Cellular tensegrity: defining new rules of biological design that govern the cytoskeleton. *J Cell Sci* 104: 613–627, 1993.
- Ingber DE. The architecture of life. *Sci Am* 278: 48–57, 1998.
- Ingber DE. Tensegrity: the architectural basis of cellular mechanotransduction. *Annu Rev Physiol* 59: 575–599, 1997.
- Janmey PA, Euteneuer U, Traub P, and Schliwa M. Viscoelastic properties of vimentin compared with other filamentous biopolymer networks. *J Cell Biol* 113: 155–160, 1991.
- Jung HI, Shin I, Park YM, Kang KW, and Ha KS. Colchicine activates actin polymerization by microtubule depolymerization. *Mol Cell* 7: 431–437, 1997.
- Katoh K, Kano Y, Masuda M, Onishi H, and Fujiwara K. Isolation and contraction of the stress fiber. *Mol Biol Cell* 9: 1919–1938, 1998.
- Keller HU and Niggli V. Colchicine-induced stimulation of PMN motility related to cytoskeletal changes in actin,  $\alpha$ -actinin, and myosin. *Cell Motil Cytoskeleton* 25: 10–18, 1993.
- Kolodney MS and Elson EL. Contraction due to microtubule disruption is associated with increased phosphorylation of myosin regulatory light chain. *Proc Natl Acad Sci USA* 92: 10252–10256, 1995.
- Kolodney MS and Wysolmerski RB. Isometric contraction by fibroblasts and endothelial cells in tissue culture: a quantitative study. *J Cell Biol* 117: 73–82, 1992.
- Kurachi M, Hoshi M, and Tashiro H. Buckling of single microtubule by optical trapping forces: direct measurement of microtubule rigidity. *Cell Motil Cytoskeleton* 30: 221–228, 1995.
- Leite R and Webb RC. Microtubule disruption potentiates phenylephrine-induced vasoconstriction in rat mesenteric arterial bed. *Eur J Pharmacol* 351: R1–R3, 1998.
- Linari M, Dobbie I, Reconditi M, Koubassova N, Irving M, Piazzesi G, and Lombardi V. The stiffness of skeletal muscle in isometric contraction and rigor: the fraction of myosin heads bound to actin. *Biophys J* 74: 2459–2473, 1998.
- Ma L, Xu J, Coulombe PA, and Wirtz D. Keratin filament suspensions show unique micromechanical properties. *J Biol Chem* 274: 19145–19151, 1999.
- MacMahon TA. *Muscles, Reflexes, and Locomotion*. Princeton, NJ: Princeton Univ. Press, 1984.
- Mooney DJ, Hansen LK, Langer R, Vacanti JP, and Ingber DE. Extracellular matrix controls tubulin monomer levels in hepatocytes. *Mol Biol Cell* 5: 1281–1288, 1994.
- Paul RJ, Bowman P, and Kolodney MS. Effects of microtubule disruption on force, velocity, stiffness and  $[\text{Ca}^{2+}]_i$  in porcine coronary arteries. *Am J Physiol Heart Circ Physiol* 279: H2493–H2501, 2000.
- Pelham RJ Jr and Wang YL. Cell locomotion and focal adhesions are regulated by substrate flexibility. *Proc Natl Acad Sci USA* 94: 13661–13665, 1997.
- Platts SH, Falcone JC, Holton WT, Hill MA, and Meininger GA. Alteration of microtubule polymerization modulates arteriolar vasomotor tone. *Am J Physiol Heart Circ Physiol* 277: H100–H106, 1999.
- Putnam AJ, Cunningham JJ, Dennis RG, Linderman JJ, and Mooney DJ. Microtubule assembly is regulated by externally applied strain in cultured smooth muscle cells. *J Cell Sci* 111: 3379–3387, 1998.
- Sheridan BC, McIntyre RC Jr, Meldrum DR, Cleveland JC Jr, Agrafojo J, Banerjee A, Harken AH, and Fullerton DA. Microtubules regulate pulmonary vascular smooth muscle contraction. *J Surg Res* 62: 284–287, 1996.
- Stamenović D and Coughlin MF. The role of prestress and architecture of the cytoskeleton and deformability of cytoskeletal filaments in mechanics of adherent cells: a quantitative analysis. *J Theor Biol* 201: 63–74, 1999.
- Svitkina TM, Verkhovsky AB, and Borisy GG. Plectin side-arms interaction of intermediate filaments with microtubules and other components of the cytoskeleton. *J Cell Biol* 135: 991–1007, 1996.
- Timoshenko SP and Gere JM. *Theory of Elastic Stability* (2nd ed.). New York: McGraw-Hill, 1988.
- Venier P, Maggs AC, Carlier MF, and Pantaloni D. Analysis of microtubule rigidity using hydrodynamic flow and thermal fluctuations. *J Biol Chem* 269: 13353–13360, 1994.
- Wang HB, Dembo M, and Wang YL. Substrate flexibility regulates growth and apoptosis of normal but not transformed cells. *Am J Physiol Cell Physiol* 279: C1345–C1350, 2000.
- Wang N, Naruse K, Stamenović D, Fredberg JJ, Mijailovich SM, Tolić-Nørrelykke IM, Polte T, Mannix R, and Ingber DE. Mechanical behavior of living cells consistent with the tensegrity model. *Proc Natl Acad Sci USA* 98: 7765–7770, 2001.

41. **Wang N and Stamenović D.** Contribution of intermediate filaments to cell stiffness, stiffening, and growth. *Am J Physiol Cell Physiol* 279: C188–C194, 2000.
42. **Wang N, Tolić-Nørrelykke IM, Chen J, Mijailovich SM, Butler JP, Fredberg JJ, and Stamenović D.** Cell prestress. I. Stiffness and prestress are closely associated in contractile adherent cells. *Am J Physiol Cell Physiol* 282: C606–C616, 2002.
43. **Warshaw DM.** The in vitro motility assay: a window into myosin molecular motor. *News Physiol Sci* 11: 1–7, 1996.
44. **Waterman-Storer CM and Salmon ED.** Actomyosin-based retrograde flow of microtubules in the lamella of migrating epithelial cells influences microtubule dynamic instability and turnover is associated with microtubule breakage and treadmilling. *J Cell Biol* 139: 417–434, 1997.

